Quantum Disordered Phase near the Mott Transition in the Staggered-Flux Hubbard Model on a Square Lattice

Chia-Chen Chang and Richard T. Scalettar
Department of Physics, University of California, Davis, Davis, California 95616, USA
(Received 17 April 2012; published 13 July 2012)

We investigate ground state properties of the half-filled staggered-flux Hubbard model on a square lattice. Energy gaps to charge and spin excitations and magnetic as well as dimer orders are calculated as a function of interaction strength U/t by means of a constrained-path quantum Monte Carlo method. It is found that the system is a semimetal at $U/t \lesssim 5.6$ and a Mott insulator, with long-range antiferromagnetic order, at $U/t \gtrsim 6.6$. In the range $5.6 \lesssim U/t \lesssim 6.6$, the ground state is a correlated insulator where both magnetic and dimer orders are absent. Furthermore, spin excitation in the intermediate phase appears to be gapless, and the measured spin-spin correlation function exhibits power-law decaying behavior. The data suggest that the nonmagnetic ground state is a possible candidate for the putative algebraic spin liquid.

DOI: 10.1103/PhysRevLett.109.026404 PACS numbers: 71.10.Fd, 02.70.Ss, 75.10.Lp, 75.40.Mg

At sufficiently low temperatures, condensed matter systems have a tendency to undergo phase transitions and develop long range order which reflects broken symmetry [1]. In a two-dimensional antiferromagnet, however, Anderson recognized that the system could have a ground state that avoids all spontaneous symmetry breaking and does not have magnetic order even at zero temperature [2]. Anderson's discovery, in conjunction with many subsequent theoretical investigations, uncovered a new class of matter, named spin liquids, that go beyond Landau's paradigm. Most notably, in contrast to conventional symmetry breaking, spin liquids possess topological orders that cannot be characterized by local order parameters and carry fractionalized excitations [3].

Model Hamiltonians have played an important role in realizing such exotic spin liquid states [4,5]. Evidence of spin liquid phases has been found in the spin 1/2 Heisenberg model on triangular lattices [6], square lattices with frustration [7–9], and kagome lattices [10]. In these geometrically frustrated systems [11], antiferromagnetic (AF) orders are suppressed by strong quantum fluctuations. In addition to spin systems, there is also progress using the Hubbard model which contains spin and charge degrees of freedom. Spin liquid ground states have been identified in the model on anisotropic triangular lattices [12] and on bipartite honeycomb lattices [13].

In this Letter, we examine ground state properties of the half-filled staggered-flux Hubbard model (SFHM) on a square lattice. As will be seen later, low energy physics in the SFHM is described by Dirac fermions, similar to those found in the Hubbard model on honeycomb lattices [13]. The model is defined by the Hamiltonian

$$H = -\sum_{\langle \mathbf{ij}\rangle,\sigma} (t_{\mathbf{ij}} c^{\dagger}_{\mathbf{i}\sigma} c_{\mathbf{j}\sigma} + t_{\mathbf{ji}} c^{\dagger}_{\mathbf{j}\sigma} c_{\mathbf{i}\sigma}) + U \sum_{\mathbf{i}} \left(n_{\mathbf{i}\uparrow} - \frac{1}{2}\right)\left(n_{\mathbf{i}\downarrow} - \frac{1}{2}\right), \quad (1)$$

where $t_{\mathbf{ij}} = te^{i\theta_{\mathbf{ij}}}$ is the nearest-neighbor hopping and we set $t = 1$ throughout this Letter. The operator $c^{\dagger}_{\mathbf{i}\sigma}$ ($c_{\mathbf{i}\sigma}$) creates (annihilates) an electron with spin $\sigma = \uparrow, \downarrow$ at site $\mathbf{i}$ on a lattice of size $N = L \times L$. $U > 0$ is the onsite Coulomb repulsion. We work in the canonical ensemble.

An electron gains a phase $\Phi = \sum_{\square} \theta_{\mathbf{ij}}$ when it hops around a plaquette of the square lattice. $\Phi = 0$ corresponds to the original Hubbard model. We focus on the case $\Phi = \pi$ in the present study. There is a gauge freedom in choosing $\theta_{\mathbf{ij}}$. Here, we distribute the phase Φ equally over all bonds around a plaquette and arrange the hoppings according to Fig. 1(a). This leads to a lattice with plaquettes threaded alternatively by flux Φ and $-\Phi$. At $U = 0$, the energy spectrum is $\epsilon_{\mathbf{k}} = \pm 2\sqrt{\cos^2 k_x + \cos^2 k_y}$. The two energy bands meet at the Fermi surface $\epsilon_{\mathbf{k}} = 0$ located at nodal points $\mathbf{k}_0 = (\pm\pi/2, \pm\pi/2)$, as shown in Fig. 1(b). Close to the four nodal points the energy depends linearly on $\mathbf{k}$, which is similar to the massless Dirac spectrum found on the honeycomb lattice.

Our key result is that, an intermediate nonmagnetic insulating ground state is identified between the semimetal phase at weak interaction strengths and the AF Mott insulator at strong couplings, where the hopping terms become irrelevant. The calculated dimer correlation function shows that columnar valence bond order is also absent in the intermediate phase. These results seem to indicate that the nonmagnetic insulating phase is a candidate for the putative algebraic spin liquid ground state. Therefore, our work suggests that recent progress in optical lattice experiments [14] might provide a promising way of simulating the model.

The SFHM is solved numerically by means of the constrained-path quantum Monte Carlo method [15]. Details of the method are described in the Supplemental Material [16]. We begin with the results for the charge excitation gap. In the canonical ensemble, the charge gap at half filling can be defined as [17]

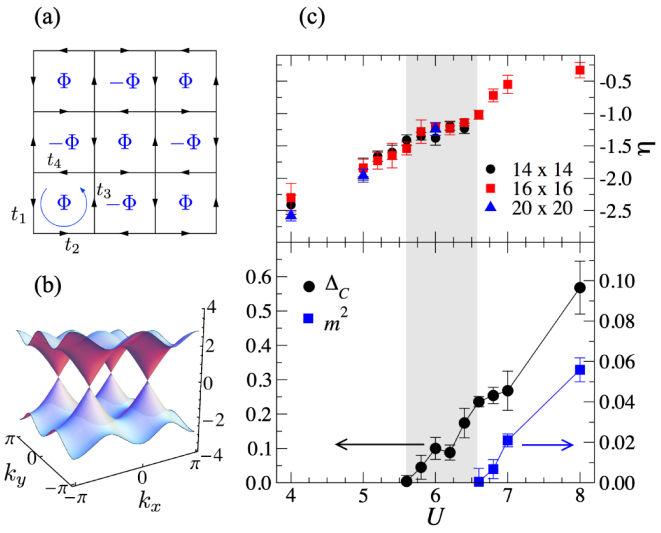

FIG. 1 (color online). (a) Arrangement of hopping amplitudes on a square lattice. The phase $\Phi = \pi$ is distributed equally so that $t_1 = t_2 = t_3 = t_4 = e^{i\Phi/4}$. (b) Band structure of the tight-binding Hamiltonian. (c) Top panel: power law exponent η extracted from fits to staggered spin-spin correlation functions. Bottom panel: thermodynamic limit charge gap Δ_C and magnetic moment m^2 (see text for definition). The shaded region indicates the nonmagnetic insulating phase.

$$\Delta_C(L) = \frac{1}{2}\left[E_g\left(\frac{N}{2}-1,\frac{N}{2}-1\right) - E_g\left(\frac{N}{2},\frac{N}{2}\right)\right], \quad (2)$$

which is the energy cost of removing a pair of electrons from the half-filled ground state while keeping the system in the $S^z_{\rm tot} = 0$ sector. We measure $\Delta_C(L)$ as a function of the interaction strength U on lattices with linear dimension up to $L = 14$. As shown in the inset of Fig. 2(a), the charge gap increases with U on finite lattices. To pinpoint the critical interaction strength where the system turns into an insulator, we extrapolate $\Delta_C(L)$ at fixed U to the thermodynamic limit $L \to \infty$ using the ansatz: $\Delta_C(L)/L^2 = \Delta_C(\infty) + f(L)$, where $f(L)$ is a polynomial in L^{-1} that satisfies $f(L \to \infty) \to 0$. In a gapped or ordered phase, $f(L)$ is typically a linear function of L^{-1} [17]. However, to take into account both gapped and gapless cases, we choose $f(L)$ to be a second order polynomial in L^{-1}. This functional form is also implemented in previous works, most recently in Refs. [8,9,13]. The results, shown in the inset of Fig. 2(a), indicate that the system is gapped for $U \gtrsim 5.6$.

In addition to the charge excitation gap, AF long-range order is another essential feature characterizing a Mott insulator. To investigate whether there is any AF order in the ground state, we calculate the spin structure factor at the Néel wave vector $\mathbf{q}_{\rm AF} = (\pi, \pi)$

$$S(\mathbf{q}_{\rm AF}, L) = \sum_{\mathbf{r}} e^{i\mathbf{q}_{\rm AF}\cdot\mathbf{r}}\langle S^x_{\mathbf{r}}S^x_0 + S^y_{\mathbf{r}}S^y_0 + S^z_{\mathbf{r}}S^z_0\rangle, \quad (3)$$

where $S^\delta_{\mathbf{r}}$ is the spin operator along the δ direction ($\delta = x$, y, z), and $\langle S^\delta_{\mathbf{r}}S^\delta_0\rangle$ is the equal-time spin-spin correlation

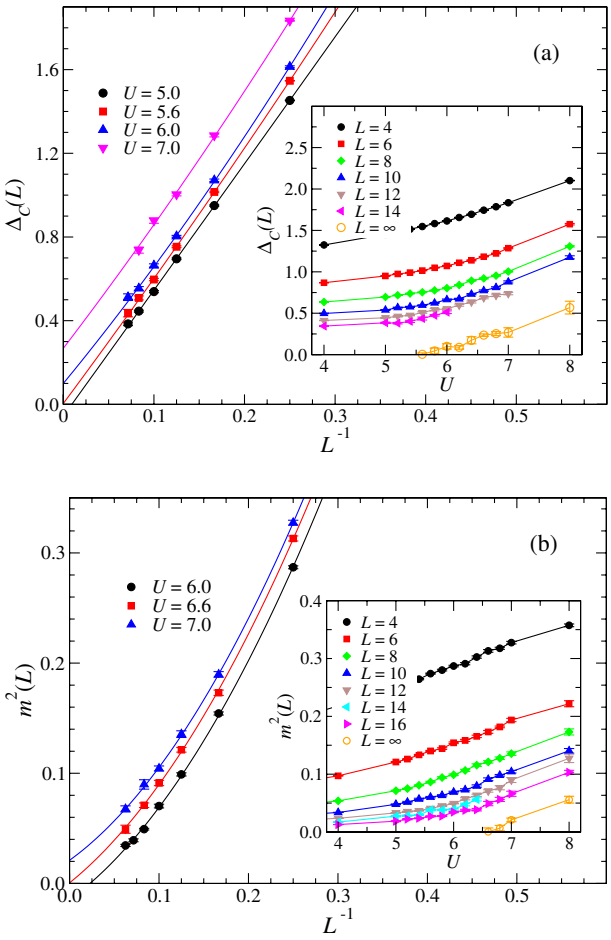

FIG. 2 (color online). (a) Extrapolation of the charge gap $\Delta_C(L)$. Solid lines represent second-order polynomial fits to the QMC data. Inset shows the charge gap $\Delta_C(L)$ as a function of U obtained for $L = 4$, 6, 8, 10, 12, 14, and extrapolated (empty circle) values. Lines are guides to the eye. (b) Finite size extrapolation of the spin structure factor $m^2(L)$. Solid lines are second-order polynomial fits to the QMC data. Inset: $m^2(L)$ versus U on finite lattices and extrapolated (empty circle) values. Lines are guides to the eye.

function. Defining $m^2(L) = S(\mathbf{q}_{\rm AF}, L)/L^2$, a magnetically ordered phase is singled by a finite $m^2(L)$ in the thermodynamic limit. The inset of Fig. 2(b) shows the results of $m^2(L)$ as a function of U on finite lattices. In order to take both magnetically ordered and disordered phases into account, we use second-order polynomials in L^{-1} [18] to fit the QMC data and extract the value of $m^2(L)$ in the $L \to \infty$ limit. It can be seen, from the inset of Fig. 2(b), that AF order kicks in at $U \gtrsim 6.6$, below which the system is in a paramagnetic phase.

Our above analysis of charge gap and magnetic order suggests that the ground state of the SFHM is a semimetal at $U \lesssim 5.6$, and becomes a Mott insulator with long-range AF order at $U \gtrsim 6.6$. Therefore, unlike the original half-filled Hubbard model that, owing to the perfect nesting on a square lattice, has AF order at arbitrarily small U [19], the

SFHM has a finite Mott transition point. A similar finite U Mott transition was reported in the square lattice Hubbard mode with uniform π flux [20]. Moreover, our results indicate that in the region $5.6 \lesssim U \lesssim 6.6$ there is an intermediate phase that is neither a semimetal nor a Mott insulator.

The absence of AF order in the intermediate phase indicates that the ground state is dominated by short-range spin correlations. At large distances, the spin correlation function could either decay exponentially or follow a power-law. To study the nature of the nonmagnetic insulating phase, we first calculate the spin excitation gap. Following Ref. [21], we write the spin gap at half filling as

$$\Delta_S(L) = E_g\left(\frac{N}{2}+1, \frac{N}{2}-1\right) - E_g\left(\frac{N}{2}, \frac{N}{2}\right), \qquad (4)$$

which measures the energy cost of flipping an electron from spin-down to spin-up. Based on confinement arguments, a gapped spin excitation implies a finite correlation length, leading to an exponentially decaying spin-spin correlation. On the other hand, the correlation function would be described by a power law if the spin excitation is gapless. We compute $\Delta_S(L)$ as a function of U on finite lattices. The spin gap results are shown in the inset of Fig. 3(a) for $5 \lesssim U \lesssim 7$. The data at a given U are then extrapolated to $L \to \infty$ using a second-order polynomial in L^{-1} to extract the spin gap in the thermodynamic limit. Typical behavior of the fits is plotted in Fig. 3(a). As expected, the extrapolated spin gap remains zero, in the gapless semimetal phase ($U \lesssim 5.6$) and in the Mott phase ($U \gtrsim 6.6$), due to the presence of gapless spin wave excitations. More importantly, $\Delta_S(L)$ also shows gapless behavior in the region $5.6 \lesssim U \lesssim 6.6$, implying that the spin-spin correlation should follow a power law at large distances.

To support this observation, we plot in Fig. 3(b) the staggered spin-spin correlation function along the x axis. It appears that $C(\mathbf{r})$, indeed, decays algebraically at large separations. Moreover, the correlation function decays more slowly with increasing U, and starts showing saturation in the Mott phase ($U \gtrsim 6.6$). In order to quantify the long-range behavior of $C(\mathbf{r})$, we fit the staggered spin correlation function to a power law $\alpha|\mathbf{r}|^{\eta}$ for $|\mathbf{r}| \geq 2$, where α and η are two fitting parameters. At $U = 0$, it is known that $C(\mathbf{r})$ decays as $|\mathbf{r}|^{-4}$ [22]. This is also demonstrated in Fig. 3(b): the fitted exponent of $C(\mathbf{r})$ for free fermions on a half-filled 24×24 is $\eta = -3.95 \pm 0.13$. The exponent η as a function of U, extracted from several half-filled lattices, is plotted in the top panel of Fig. 1(c). It can be seen, from the figure, that η immediately increases with U from its noninteracting value due to the effect of interaction. Although the data are quite scattered, the figure suggests that the exponent η increases slowly with U in the region $5.6 \lesssim U \lesssim 6.6$.

Next, we consider other order parameters proposed in Ref. [22]. The simplest scenario is the columnar valence bond solid (VBS) which breaks translational symmetry. The VBS order can be probed by measuring the dimer structure factor

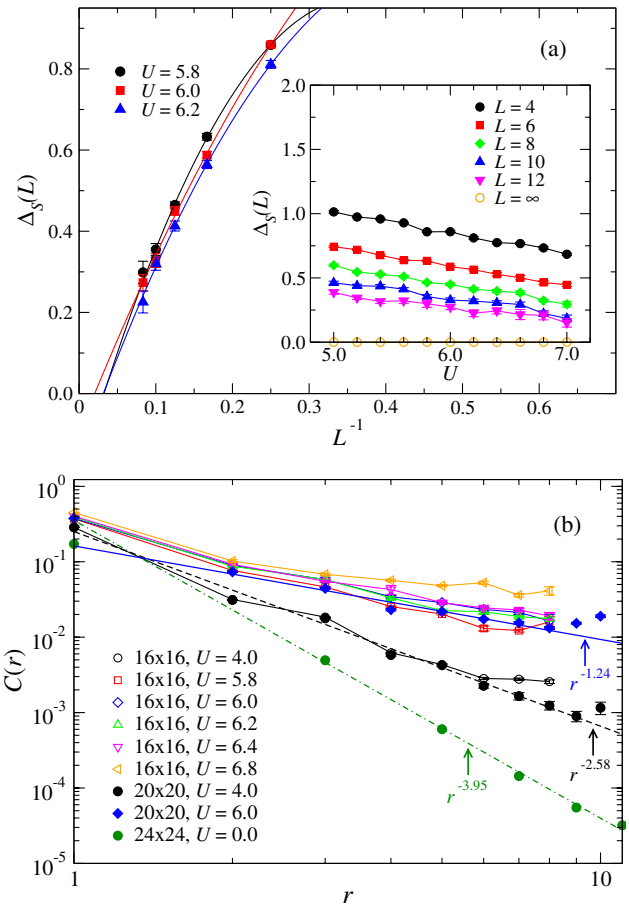

FIG. 3 (color online). (a) Finite size extrapolation of the spin gap $\Delta_S(L)$. Solid lines are second-order polynomial fits to the Monte Carlo data. The inset illustrates $\Delta_S(L)$ and its extrapolated value. Lines are guides to the eye. (b) Long-range behavior of the staggered spin-spin correlation function $C(\mathbf{r}) = (-1)^{\mathbf{r}} \times \langle S^x_{\mathbf{r}} S^x_0 + S^y_{\mathbf{r}} S^y_0 + S^z_{\mathbf{r}} S^z_0 \rangle$ obtained on $L = 16$, 20, and 24 ($U = 0$ only). Straight lines are representative power-law fits to the data: green (dot-dashed) line $L = 24$ at $U = 0$, black (dashed) line $L = 20$ at $U = 4$, and blue (solid) line $L = 20$ at $U = 6$.

$$D_{\delta\delta}(\mathbf{q}, L) = \frac{1}{N}\sum_{\mathbf{r}} e^{i\mathbf{q}\cdot\mathbf{r}} C^z_{\delta\delta}(\mathbf{r}), \qquad (5)$$

where $C^z_{\delta\delta}(\mathbf{r})$ is the z component equal-time dimer-dimer correlation function for singlet bonds along the δ direction ($\delta = x, y$)

$$C^z_{\delta\delta}(\mathbf{r}) = \langle S^z_{\mathbf{r}+\hat{\delta}} S^z_{\mathbf{r}} S^z_{\hat{\delta}} S^z_0 \rangle - \langle S^z_{\hat{\delta}} S^z_0 \rangle^2. \qquad (6)$$

In the columnar VBS state, dimers line up coherently. Therefore, $D_{\delta\delta}(\mathbf{q}, L)$ would pick up a characteristic momentum at $\mathbf{k}_{xx} = (\pi, 0)$ or $\mathbf{k}_{yy} = (0, \pi)$ for $\delta = x$ or $\delta = y$ depending on the orientation of the bonds. Indeed, $D_{\delta\delta}(\mathbf{q}, L)$ peaks at $\mathbf{k}_{\delta\delta}$ in our finite size simulations, as

shown in the Supplemental Material [16]. To extract the VBS order in the thermodynamic limit, we calculate $d^2_{\delta\delta}(L) = D_{\delta\delta}(\mathbf{k}_{\delta\delta})/N$ and extrapolate to the $L \to \infty$ limit. As shown in Figs. 4(a) and 4(b), both quantities vanish in the thermodynamic limit, implying the absence of columnar VBS order in the intermediate phase.

In addition to the columnar VBS state, another competing order proposed in Ref. [22] is the plaquette VBS order. This state is a coherent superposition of singlets formed by 4 spins located on corners of a plaquette. Given the lattice sizes studied in this Letter, however, we are not able to obtain a reliable thermodynamic estimation of the plaquette VBS order as a function of U.

A commonly adopted definition of a spin liquid is that: it is a nonmagnetic Mott insulator, in which neither spin nor lattice symmetry is broken. Based on this definition, our numerical data presented in this Letter seems to suggest an algebraic spin liquid ground state in the half-filled SFHM [23]. However, the most unambiguous evidence of a spin liquid is its fractionalized excitation [24]. Due to the nature of our method, we are not able to directly measure quantum properties of excited states. As we have mentioned previously, it is possible to simulate the SFHM with optical lattice experiment setups [14]. In such experiments, a direct method of detecting a spin liquid would be measuring the entanglement entropy (EE) [25]. Although EE does not correspond to any physical observables, it has been proposed that EE can be measured using quantum quenches [26].

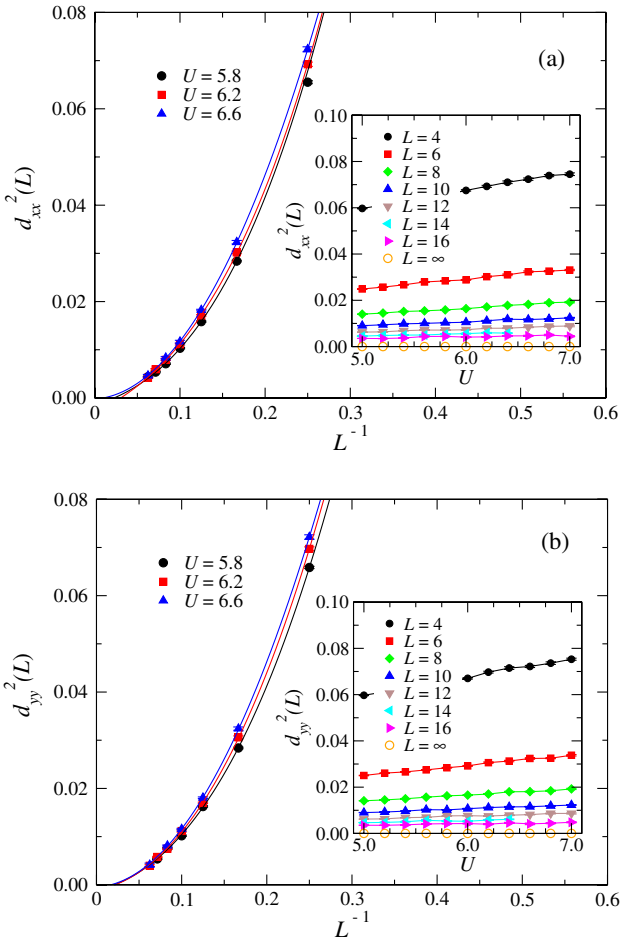

FIG. 4 (color online). Thermodynamic limit extrapolation of the columnar VBS order. In both figures, solid lines are three representative third-order polynomial fits to the Monte Carlo data. Insets show the normalized dimer structure for single bonds in x or y directions on finite size lattices. Lines are guides to the eye. The extrapolated value in the thermodynamic limit is indicated by orange (empty) circles in the insets.

In terms of the method, we note that although the half-filled staggered-flux model does not have the fermion sign problem, we deliberately keep the constrained-path approximation and calculate the ground state properties at half filling. Our benchmark data show that the error appears to be small when compared with exact answers, as shown by the benchmark data in the Supplemental Material [16]. However, it is possible that the systematic error grows with L. A recent exact QMC method, a linearized auxiliary fields Monte Carlo technique, reports that the half-filled ground state energy at $U = 4$ is $-0.859\,96(5)$ [27] per site, in the thermodynamic limit. Our method, after boundary condition averaging, gives $-0.8559(4)$ [28], corresponding to a 0.47% error. By including this systematic error, we estimate that the lower critical point, where charge gap opens, would be pushed to $U \sim 5.4 \pm 0.1$. In observable results such as correlation functions, extensive tests [15,29] show that our systematic error is small even at half filling [29] and does not affect the physics of the numerical solutions.

To summarize, we have studied ground state properties in the half-filled staggered-flux Hubbard model on a square lattice. Charge and spin excitation gaps as well as spin and dimer orders are extracted by means of the constrained-path quantum Monte Carlo method. The system is found to be a semimetal at $U \lesssim 5.6$ and an AF Mott insulator at $U \gtrsim 6.6$. In the region $5.6 \lesssim U \lesssim 6.6$, our data suggests that both AF and VBS orders are absent in the ground state. Spin excitation in this region is gapless, a result that is consistent with the calculated staggered spin-spin correlation function, which shows power-law decaying behavior at large distances.

We thank Professor Rajiv R. P. Singh and Professor Shiwei Zhang for helpful comments. C. C. would like to thank Professor Hong Yao for illuminating discussions. This research was supported by the DOE SciDAC (Grant No. DOE-DE-FC0206ER25793) and NSF PIF (Grant No. NSF-PHY-1005503) Programs. Computations were performed on Kraken at the National Institute for Computational Sciences.

[1] L. Landau, Phys. Z. Sowjetunion **11**, 26 (1937).
[2] P. Anderson, Mater. Res. Bull. **8**, 153 (1973).
[3] X.-G. Wen, Phys. Rev. B **65**, 165113 (2002).
[4] J. Marston and C. Zeng, J. Appl. Phys. **69**, 5962 (1991).

[5] S. Sachdev, Phys. Rev. B **45**, 12 377 (1992).
[6] S. Yunoki and S. Sorella, Phys. Rev. B **74**, 014408 (2006).
[7] A. Sandvik, Phys. Rev. Lett. **98**, 227202 (2007).
[8] H.-C. Jiang, H. Yao, and L. Balents, arXiv:1112.2241.
[9] L. Wang, Z.-C. Gu, F. Verstraete, and X.-G. Wen, arXiv:1112.3331.
[10] S. Yan, D. A. Huse, and S. R. White, Science **332**, 1173 (2011).
[11] L. Balents, Nature (London) **464**, 199 (2010).
[12] H. Morita, S. Watanabe, and M. Imada, J. Phys. Soc. Jpn. **71**, 2109 (2002).
[13] Z. Meng, T. Lang, S. Wessel, F. Assaad, and A. Muramatsu, Nature (London) **464**, 847 (2010).
[14] M. Aidelsburger, M. Atala, S. Nascimbène, S. Trotzky, Y. A. Chen, and I. Bloch, Phys. Rev. Lett. **107**, 255301 (2011).
[15] S. Zhang, J. Carlson, and J. E. Gubernatis, Phys. Rev. Lett. **74**, 3652 (1995); Phys. Rev. B **55**, 7464 (1997).
[16] See Supplemental Material at http://link.aps.org/supplemental/10.1103/PhysRevLett.109.026404 for (in the first part) a summary of the constrained-path quantum Monte Carlo method used in this Letter and (in the second part) a brief discussion of typical behaviors of dimer-dimer correlation function and dimer-dimer structure factor.
[17] N. Furukawa and M. Imada, J. Phys. Soc. Jpn. **61**, 3331 (1992).
[18] D. A. Huse, Phys. Rev. B **37**, 2380 (1988).
[19] J. E. Hirsch, Phys. Rev. B **31**, 4403 (1985).
[20] Y. Otsuka and Y. Hatsugai, Phys. Rev. B **65**, 073101 (2002).
[21] R. Noack, S. White, and D. Scalapino, Europhys. Lett. **30**, 163 (1995).
[22] M. Hermele, T. Senthil, and M. P. A. Fisher, Phys. Rev. B **72**, 104404 (2005).
[23] In the square lattice Hubbard model with uniform π flux, it has been suggested that a nodal spin liquid might exist. For example: G.-Y. Sun and S.-P. Kou, Europhys. Lett. **87**, 67002 (2009); S.-P. Kou, L.-F. Liu, J. He, and Y.-J. Wu, Eur. Phys. J. B **81**, 165 (2011).
[24] G. Misguich, in *Introduction to Frustrated Magnetism*, edited by C. Lacroix, P. Mendels, and F. Mila (Springer-Verlag, Berlin, 2011) pp. 407–435.
[25] Y. Zhang, T. Grover, and A. Vishwanath, Phys. Rev. Lett. **107**, 067202 (2011).
[26] J. Cardy, Phys. Rev. Lett. **106**, 150404 (2011).
[27] S. Sorella, Phys. Rev. B **84**, 241110(R) (2011).
[28] C.-C. Chang and S. Zhang, Phys. Rev. B **78**, 165101 (2008).
[29] S. Zhang, J. Carlson, and J. E. Gubernatis, Phys. Rev. Lett. **78**, 4486 (1997).